Canadian Science Publishing
NRC Research Press journals | Publishing Services

Canadian Geotechnical Journal
Revue canadienne de géotechnique

Influence of cross-correlation between soil parameters on probability of failure of simple cohesive and c-phi slopes

Journal:	*Canadian Geotechnical Journal*
Manuscript ID	cgj-2015-0109.R1
Manuscript Type:	Article
Date Submitted by the Author:	11-Aug-2015
Complete List of Authors:	Javankhoshdel, Sina; Queen's University, Civil Engineering Dept Bathurst, Richard; Queens University/Royal Military College,
Keyword:	slope stability, probabilistic analysis, cross-correlation, Monte Carlo simulation, stability charts

MS. cgj-2014-0292R2 final (clean) text only November 2015

Influence of cross-correlation between soil parameters on probability of failure of simple cohesive and c-ϕ slopes

Sina Javankhoshdel[1]

Richard J. Bathurst[2]

[1] PhD candidate
GeoEngineering Centre at Queen's-RMC
Department of Civil Engineering
Ellis Hall
Queens University
Kingston, Ontario, K7L 3N6 CANADA

Phone: (613) 541-6000 (ext. 6347)
Email: s.javan.khoshdel@queensu.ca

[2] Professor and Research Director **(corresponding author)**
GeoEngineering Centre at Queen's-RMC
Department of Civil Engineering, 13 General Crerar, Sawyer Building, Room 2414, Royal Military College of Canada, Kingston, Ontario, K7K 7B4 CANADA

Phone: (613) 541-6000 (ext. 6479/6347/6391)
Email: bathurst-r@rmc.ca

ABSTRACT

The paper focuses on the calculation of probability of failure of simple unreinforced slopes and the influence of the magnitude of cross-correlation between soil parameters on numerical outcomes. A general closed-form solution for cohesive slopes with cross-correlation between cohesion and unit weight was investigated and results compared with cases without cross-correlation. Negative cross-correlations between cohesion and friction angle and positive cross-correlations between cohesion and unit weight, and friction angle and unit weight were considered in the current study. The factors of safety and probabilities of failure for the slopes with uncorrelated soil properties were obtained using probabilistic slope stability design charts previously reported by the writers. Results for cohesive soil slopes and positive cross-correlation between cohesion and unit weight are shown to decrease probability of failure. Probability of failure also decreased for increasing negative cross-correlation between cohesion and friction angle, and increasing positive correlation between cohesion and unit weight, and friction angle and unit weight. Probabilistic slope stability design charts presented by the writers in an earlier publication are extended to include c-ϕ soil slopes with and without cross-correlation between soil input parameters. An important outcome of the work presented here is that cross-correlation between random values of soil properties can reduce the probability of failure for simple slope cases. Hence, previous probabilistic design charts by the writers for simple soil slopes with uncorrelated soil properties are conservative (safe) for design. This study also provides one explanation why slope stability analyses using uncorrelated soil properties can predict unreasonably high probabilities of failure when conventional estimates of factor of safety suggest a stable slope.

Keywords: Slope stability; Probabilistic analysis; cross-correlation; Monte Carlo simulation

INTRODUCTION

Slope stability charts are used routinely to estimate the conventional factor of safety of unreinforced slopes with isotropic, homogeneous soil properties and simple geometry. Design charts by **Taylor (1937)**, **Michalowski (2002)**, **Baker (2003)** and **Steward et al. (2011)** are just a few examples to calculate the factor of safety for cohesive (c) and cohesive-frictional (c–ϕ) soil

slopes. These design charts are based on the deterministic kinematic approach of limit analyses or deterministic limit equilibrium methods of analysis. An important limitation of deterministic methods for conventional slope stability analyses is that nominal similar slopes may have the same factor of safety but different probabilities of failure. This is attributed to random and spatial variability of slope soil properties.

Javankhoshdel and Bathurst (2014) presented a closed-form solution to calculate probability of failure for cohesive soil slopes ($c = s_u > 0$, $\phi = \phi_u = 0$). The probability of failure is calculated directly using the mean value of the factor of safety and coefficient of variation (COV) of soil cohesion and unit weight (γ). A similar equation for the case of random variability in cohesive soil strength only has been published by **Griffiths and Fenton (2004)**.

Javankhoshdel and Bathurst (2014) also produced a series of slope stability charts for c–ϕ soils that have the advantage that they do not require an iterative approach to calculate the factor of safety, and they include in the same chart an estimate of the probability of failure using the random variability of soil properties expressed by the coefficient of variation (COV) as inputs. The ranges of COV values in these charts are $0.1 \leq COV_c \leq 0.5$, $0.1 \leq COV_\phi \leq 0.2$ and $COV_\gamma \leq 0.1$ for soil cohesion, friction angle and unit weight, respectively. Recall that coefficient of variation (COV) is the ratio of standard deviation to mean value.

In the related prior work for cohesive and c–ϕ soil cases by the writers, the implications of possible correlations between input parameters on probability of failure outcomes were recognized and some quantitative examples provided.

Possible correlations between random values of shear strength parameters that can influence probability of failure estimates for slopes have been noted by **Nguyen and Chowdhury (1985)**. These correlations are quantified by the cross-correlation coefficient (ρ). Negative correlations between c and ϕ have been reported from laboratory measurements (**Lumb 1970; Yucemen et al. 1973; Cherubini 1997, 2000; Forrest and Orr 2010; Hata et al. 2011**). A negative cross-correlation coefficient is computed when the cohesive soil strength component (c) decreases with increasing friction angle (ϕ). The uncertainty (or spread) in estimates of soil shear strength is

smaller when there is a negative correlation between random values of c and ϕ compared to the case of uncorrelated random values. **Le (2014), Griffiths et al. (2009)** and **Allahverdizadeh et al. (2015)** investigated the effect of positive cross-correlation between c and ϕ in soil slopes with spatial variability using the random finite element method (RFEM) method.

There is little data available to quantify correlations between c and unit weight (γ), and between ϕ and γ (**Matsuo and Kuroda 1974; Parker et al. 2008**). A positive correlation coefficient for these random variables is most often assumed in the literature (**Chowdhury and Xu 1993; Low and Tang 1997; Sivakumar Babu and Srivastava 2007**).

In the current study the influence of cross-correlation of random soil parameters on probability of failure of simple slopes is examined in more depth. For the case of cohesive soil slopes, the influence of positive cross-correlation between cohesion and unit weight is investigated using a closed-form solution and also numerically using Monte Carlo simulation. For the case of c−ϕ soils, the effect of negative cross-correlation between strength parameters (c and ϕ) and negative and positive correlation between c and γ, ϕ and γ , respectively, are also investigated using Monte Carlo simulation. New probabilistic slope stability design charts for c-ϕ soils similar to the charts published by **Javankhoshdel and Bathurst (2014)** are presented. These new charts allow the user to calculate factor of safety and probability of failure with and without considering negative cross-correlation between c and ϕ and positive cross-correlation between c and γ , and ϕ and γ.

The results of analyses presented in this study and the companion paper by **Javankhoshdel and Bathurst (2014)** are restricted to the case of random variability of soil parameters. The influence of spatial variability of soil parameters is not considered. The analyses results in the earlier and current study apply to idealized simple slope geometries and soil conditions. Hence, the real world influence of pore water pressure, soil stratigraphy and the like are not considered. This was done purposely to focus attention on the influence of statistical characteristics of random soil properties on probability of failure.

The next section provides a summary explanation of how cross-correlations between random variables can be formulated for use in Monte Carlo simulations.

CROSS-CORRELATION BETWEEN INPUT PARAMETERS

General

The Monte Carlo simulation technique can be used to generate the probability distribution of a function of multiple random variables from the probability distributions of the contributing random variables. A random variable X can be computed as:

$$X = \sigma Z + \mu \quad [1]$$

Here, Z is the standard variable (mean $\mu = 0$ and standard deviation $\sigma = 1$) corresponding to the variable X. The normal probability distribution of each random variable is considered to be known. Values of Z can be calculated using the standard normal distribution function Φ (NORMSDIST) in Excel.

Covariance matrix

In general, a multivariate Gaussian (normal) distribution of n random variables, denoted by $X = (X_1, X_2, \ldots, X_n)$, has a symmetrical n x n covariance matrix given by:

$$\Lambda = [\mathrm{cvar}_{ij}] = \begin{bmatrix} \mathrm{cvar}_{11} & \mathrm{cvar}_{12} & \ldots & \mathrm{cvar}_{1n} \\ \mathrm{cvar}_{21} & \mathrm{cvar}_{22} & \ldots & \mathrm{cvar}_{2n} \\ \ldots & \ldots & & \ldots \\ \mathrm{cvar}_{n1} & \mathrm{cvar}_{n2} & \ldots & \mathrm{cvar}_{nn} \end{bmatrix} \quad [2]$$

where the element cvar_{ij} is the covariance of random variables X_i and X_j expressed as:

$$cvar_{ij} = COVARIANCE(X_i, X_j) \quad [3]$$

The terms on the main diagonal are the squares of the standard deviation (variance). If all random variables are uncorrelated, then all terms except those on the main diagonal are zero.

Based on probability theory, if two normal random variables X_i and X_j are correlated, then the cross-correlation coefficient (ρ) between X_i and X_j expressed as ρ_{X_i, X_j} can be calculated as:

$$\rho = \rho_{X_i,X_j} = \frac{cvar_{X_i,X_j}}{\sigma_{X_i}\sigma_{X_j}} \quad [4]$$

Here, σ_{X_i} and σ_{X_j} are the standard deviation of the random variables X_i and X_j, respectively. Therefore the covariance matrix can be rewritten as:

$$\Lambda = [\sigma_{ij}] = \begin{bmatrix} \sigma_1^2 & \rho_{1,2}\sigma_1\sigma_2 & \cdots & \rho_{1,n}\sigma_1\sigma_n \\ \rho_{2,1}\sigma_2\sigma_1 & \sigma_2^2 & \cdots & \rho_{2,n}\sigma_2\sigma_n \\ \vdots & \vdots & & \vdots \\ \rho_{n,1}\sigma_n\sigma_1 & \rho_{n,2}\sigma_n\sigma_2 & \cdots & \sigma_n^2 \end{bmatrix}$$

[5]

In this study the covariance matrix with 3 x 3 elements was used matching the case for three random variables. Each pair of variables is cross-correlated with ρ denoted as

ρ_1: Cross-correlation between cohesion and friction angle

ρ_2: Cross-correlation between cohesion and unit weight

ρ_3: Cross-correlation between friction angle and unit weight

The covariance matrix can now be defined as:

$$\Lambda = \begin{bmatrix} \sigma_c^2 & \rho_1\sigma_c\sigma_\phi & \rho_2\sigma_c\sigma_\gamma \\ \rho_1\sigma_\phi\sigma_c & \sigma_\phi^2 & \rho_3\sigma_\phi\sigma_\gamma \\ \rho_2\sigma_\gamma\sigma_c & \rho_3\sigma_\gamma\sigma_\phi & \sigma_\gamma^2 \end{bmatrix} \quad [6]$$

Using this covariance matrix and mathematical developments reported by **Nguyen and Chowdhury (1985)**, three correlated random variables can be computed as follows:

$$c = \sigma_c Z_1 + \mu_c \quad [7]$$

$$\phi = \rho_1\sigma_\phi Z_1 + \sigma_\phi\sqrt{1-\rho_1^2}Z_2 + \mu_\phi \quad [8]$$

$$\gamma = \rho_2\sigma_\gamma Z_1 + \frac{\sigma_\gamma(\rho_3-\rho_1\rho_2)}{\sqrt{1-\rho_1^2}}Z_2 + \sigma_\gamma\sqrt{1-\rho_2^2+\frac{(\rho_3-\rho_1\rho_2)^2}{1-\rho_1^2}}Z_3 + \mu_\gamma \quad [9]$$

Here, σ_c, σ_ϕ and σ_γ are the standard deviations of the three random variables, and Z_1, Z_2 and Z_3 are the corresponding standard variables.

The above development is based on normal distribution of input parameters. In this study all input parameters are assumed to be lognormal distributed. Therefore, to use the above equations, random variables and cross-correlation coefficients must be transformed from lognormal to normal values. Transformation equations (e.g. for ϕ) are as follows:

$$\mu_{\ln\phi} = \ln(\mu_\phi) - \frac{1}{2}\sigma^2_{\ln\phi} \quad [10]$$

$$\sigma^2_{\ln\phi} = \ln(1 + COV^2_\phi) \quad [11]$$

The cross-correlation coefficient for c and ϕ is as follows:

$$\rho_1(\ln\phi, \ln c) = \frac{\ln(1+\rho_1 COV_\phi COV_c)}{\sqrt{\ln(1+COV_\phi{}^2)\ln(1+COV_c{}^2)}} \quad [12]$$

Here, $\sigma_{\ln\phi}$ and $\mu_{\ln\phi}$ are standard deviation and the mean value of the lognormal values of ϕ. Quantities COV_ϕ and μ_ϕ are coefficient of variation and the mean value of ϕ, and COV_c is the coefficient of variation of c. Quantity $\rho_1(\ln\phi, \ln c)$ is the cross-correlation coefficient for lognormal values of c and ϕ, and ρ_1 is the cross-correlation coefficient for c and ϕ introduced earlier.

Analytical developments presented here are simplified for the case of cohesive soil slopes where only random variables s_u and γ can be correlated. Here, c is replaced by s_u denoting undrained soil shear strength. For this case, $\rho_1 = \rho_3 = 0$ and the covariance matrix is 2 x 2 as follows:

$$\Lambda = \begin{bmatrix} \sigma_{su}{}^2 & \rho_2\sigma_{su}\sigma_\gamma \\ \rho_2\sigma_\gamma\sigma_{su} & \sigma_\gamma{}^2 \end{bmatrix} \quad [13]$$

Random variables s_u and γ are now expressed by the following equations:

$$s_u = \sigma_{su} Z_1 + \mu_{su} \quad [14]$$

$$\gamma = \rho\sigma_\gamma Z_1 + \sigma_\gamma\sqrt{1-\rho^2}Z_3 + \mu_\gamma \quad [15]$$

where $\rho = \rho_2$ is used to simplify presentation.

Previous researchers have assumed values of cross-correlation coefficient (ρ_1) between c and ϕ of -0.7 and -0.2, and (ρ_2) between c and γ and (ρ_3) between ϕ and γ of 0.2 and 0.7 (**Wu 2013; Sivakumar Babu and Srivastava 2007**). As mentioned in the introduction, there is little data available to confirm that these ranges of cross-correlation coefficient for c and γ, and ϕ and γ are reasonable. However, in the current investigation similar ranges of ρ were used in order to identify trends in analysis outcomes.

Ching and Phoon (2012) used the same procedure to create a multivariate probability distribution function for five correlated soil parameters for cohesive soil slopes and showed that there is a cross-correlation of about 0.7 between undrained cohesion and effective stress which is comparable to the upper-bound value of ρ_2 reported in the literature.

COUPLED BISHOP'S CIRCULAR SLIP ANALYSIS AND MONTE CARLO SIMULATION

In each Monte Carlo realization, three different random numbers between 0 and 1 are generated. Next, standard normal variables (Z_1, Z_2 and Z_3) are calculated based on the standard deviation and mean value of the random variables. Then, random variables for c, ϕ and γ are computed using **Equations 7-9**. For each set of random input parameters the factor of safety is calculated for all slip surfaces using the Simplified Bishop's circular slip analysis method and the minimum factor of safety recorded for that set of random variables. Finally, the probability of failure from all Monte Carlo simulations is computed as the number of factors of safety less than one divided by the total number of Monte Carlo simulations. This procedure was implemented in a Visual Basic code that coupled the Monte Carlo simulation with the Simplified Bishop's circular slip

method. In this study, 10000 and 5000 Monte Carlo simulations were used for models with three and two random variables, respectively.

ANALYTICAL METHOD FOR COHESIVE SOIL SLOPES

The probabilistic slope stability design chart developed for purely cohesive soil cases by **Javankhoshdel and Bathurst (2014)** uses the factor of safety (F_s) computed from Taylor's chart as the independent (input) parameter. The factor of safety is calculated as:

$$F_s = \frac{s_u}{\gamma H N_s} \quad [16]$$

where s_u is undrained shear strength, γ is total unit weight, H is the height of slope and N_s is a stability number which is a function of slope angle (α) and depth factor (D) where DH is the depth from slope crest to a firm stratum (**Figure 1**). Height H and slope angle α are considered to be deterministic.

From probability theory, probability of failure ($F_s < 1$) for the case of lognormal input parameters can be expressed as:

$$P_f = p\left[F_s < 1\right] = \Phi\left(\frac{-\mu_{\ln Fs}}{\sigma_{\ln Fs}}\right) \quad [17]$$

where, Φ is the cumulative standard normal distribution function, and $\mu_{\ln Fs}$ and $\sigma_{\ln Fs}$ are the mean and standard deviation of the normally distributed random variable $\ln F_s$. In this development, the factor of safety F_s is defined by **Equation 16**. If s_u and γ in **Equation 16** are correlated and lognormal distributed random variables with mean values of μ_{su} and μ_γ, respectively, and N_s and

H are constant values, then the mean value and standard deviation of logarithmic values of F_s can be calculated using general formulations published by **Ang and Tang (1984)**, hence:

$$\mu_{lnFs} = \mu_{lnsu} - \mu_{ln\gamma} - \ln(HN_s) \quad [18]$$

$$\sigma_{lnFs}{}^2 = \sigma_{lnsu}^2 + \sigma_{ln\gamma}^2 - 2\mathrm{cvar}(\ln s_u, \ln\gamma) \quad [19]$$

Here, μ_{lnsu} and $\mu_{ln\gamma}$ are mean values of $\ln s_u$ and $\ln\gamma$, respectively, σ_{lnsu} and $\sigma_{ln\gamma}$ are their corresponding standard deviations, and $\mathrm{cvar}(\ln s_u, \ln\gamma)$ is covariance between $\ln s_u$ and $\ln\gamma$. These parameters can be calculated as follows using the transformations introduced earlier:

$$\sigma_{lnsu}^2 = \ln(1 + COV_{su}^2) \quad [20]$$

$$\mu_{lnsu} = \ln(\mu_{su}) - \frac{1}{2}\sigma_{lnsu}^2 \quad [21]$$

$$\sigma_{ln\gamma}^2 = \ln(1 + COV_{\gamma}^2) \quad [22]$$

$$\mu_{ln\gamma} = \ln(\mu_{\gamma}) - \frac{1}{2}\sigma_{ln\gamma}^2 \quad [23]$$

$$\mathrm{cvar}(\ln s_u, \ln\gamma) = \rho(\ln s_u, \ln\gamma)\, \sigma_{lnsu}\sigma_{ln\gamma} \quad [24]$$

Parameters COV_{su} and COV_{γ} are coefficients of variation of variable s_u and γ, respectively. Parameter $\rho(\ln s_u, \ln\gamma)$ is the cross-correlation coefficient between $\ln s_u$ and $\ln\gamma$ and is defined as:

$$\rho(\ln s_u, \ln\gamma) = \frac{\ln(1+\rho COV_{su} COV_{\gamma})}{\sigma_{\ln su}\sigma_{\ln\gamma}} \quad [25]$$

Here, ρ in the numerator is the cross-correlation coefficient between s_u and γ. Algebraic manipulation leads to the following expanded general expression for **Equation 2**:

$$P_f = p[F_s < 1] = \Phi\left(\frac{\ln\left(\sqrt{\frac{1+COV_{su}^2}{1+COV_{\gamma}^2}}/\bar{F}_S\right)}{\sqrt{\ln((1+COV_{su}^2)(1+COV_{\gamma}^2)/(1+\rho COV_{su} COV_{\gamma})^2)}}\right) \quad [26]$$

Parameter $\bar{F}_s$ is the mean factor of safety computed using mean values of s_u and γ as follows:

$$\bar{F}_s = \frac{\mu_{su}}{\mu_{\gamma} H N_s} \quad [27]$$

Equation 26 with $\rho = 0$ was used by **Javankhoshdel and Bathurst (2014)** to generate the design chart in **Figure 2** for cohesive soil slopes using the NORMSDIST function for Φ in Excel.

The solid curves plotted in **Figure 2** show results of calculations using **Equation 26** with $\rho = 0$, for a range of coefficient of variation for F_s that captures the spread in both s_u and γ values. The mean factor of safety is computed using **Equation 27** with N_s taken from Taylor's Chart (**Figure 1**). The quantity COV_{Fs} is computed using:

$$COV_{Fs} = \sqrt{COV_{su}^2 + COV_{\gamma}^2} \quad [28]$$

The range for the coefficient of variation for s_u is $COV_{su} = 0.1$ to 0.5 and for γ is $COV_{\gamma} \leq 0.1$. Hence, curves falling within the shaded area in **Figure 2** are of practical interest (i.e. between $COV_{Fs} = 0.1$ and 0.5).

EXAMPLE RESULTS

Cohesive soil slopes

Figure 3a shows the influence of cross-correlation between random values of soil cohesion (s_u) and unit weight (γ) on probability of failure (P_f). The values of the probability of failure for the same mean values of factor of safety and values of $\rho = \rho_2 = -0.7$, 0, 0.7 are shown with three combinations of $COV_{su} = 0.1$, 0.5 and 4, and constant $COV_{\gamma} = 0.1$. For $COV_{su} = 0.1$ and $COV_{su} = 0.5$, negative ρ values increase probability of failure compared to the case with $\rho = 0$, while positive ρ values decrease probability of failure. However, for $COV_{su} = 4$, negative ρ values decrease probability of failure and positive ρ values increase probability of failure. This reversal occurs when $COV_{su} = 1$ in **Equation 26**. It should be noted that the case of negative correlation between s_u and γ is of academic interest, but plotting these cases helps to identify trends in the figure plots.

In **Figure 3a**, the difference between probabilities of failure for different values of ρ is greater for lower values of COV_{su}. For example, for $F_s = 1.3$ and $COV_{su} = 0.1$, $P_f = 0.04\%$, 3.5% and 8% for $\rho = 0.7$, 0 and –0.7 respectively, while for the same $F_s = 1.3$ but for $COV_{su} = 0.5$, $P_f = 35\%$, 37% and 39% for $\rho = 0.7$, 0 and –0.7 respectively. The reason is, for lower values of COV_{su}, the magnitudes of COV_{su} and COV_{γ} are similar and the effect of cross-correlation between cohesion and unit weight on probability of failure is greater. However, for $COV_{su} = 4$, COV_{γ} is negligible compared to COV_{su} and the effect of cross-correlation between cohesion and unit weight on probability of failure is less. The trends described here are also apparent when the reliability index $\beta = -\Phi^{-1}(P_f)$ is used to quantify the margin of safety as shown in **Figure 3b**. Reliability

index rather than probability of failure is the preferred choice of parameter in reliability theory-based design codes.

The maximum possible range of the cross-correlation coefficient is $-1 < \rho < 1$. **Figures 4a** and **4b** show the influence of changing cross-correlation coefficient from –0.7 to 0.7 on probability of failure for different mean values of factor of safety using **Equation 26**. The upper bound value of ρ is close to the maximum value used by **Sivakumar Babu and Srivistava (2007)** who examined the influence of cross-correlation between the same parameters but for the case of bearing capacity of shallow foundations. In **Figure 4a**, combinations of $COV_{su} = 0.5$ and $COV_{\gamma} = 0.1$, and in **Figure 4b**, $COV_{su} = 0.2$ and $COV_{\gamma} = 0.1$ are presented. In these figures for $F_s > 1$, probability of failure decreases with increasing ρ, while for $F_s < 1$, probability of failure increases with increasing ρ. This influence results from the location of the mean values of input parameters relative to the limit state function as explained by **Griffiths et al. (2009**). In the case of $P_f < 0.5$ (mean values of F_s are on the safe side of the limit state function $F_s > 1$), increasing ρ decreases probability of failure and for $P_f > 0.5$ (when the mean values of F_s are on the unsafe side of the limit state function $F_s < 1$) increasing ρ increases the probability of failure. The explanation for this trend is related to the negative and positive sign of β when $P_f > 0.5$ and $P_f < 0.5$ respectively, and the influence ρ on the magnitude of β**.**

In **Figure 4b**, probability of failure is less than **Figure 4a** for the same value of F_s and ρ because of the lower value of $COV_{su} = 0.2$ in **Figure 4b** compared to $COV_{su} = 0.5$ in **Figure 4a**. Superimposed on these figures are the results of numerical probabilistic slope stability analysis using a Visual Basic code written by the writers to implement the coupled Simplified Bishop's circular slip analysis and Monte Carlo simulation method described earlier. The closed-form solutions and numerical results are judged to be in good agreement. This gives confidence that the numerical code used later in the paper for c-ϕ soil cases is correct based on comparison with available analytical solutions which exist only for cohesive soil slope cases with simple geometry.

Figures 4a and **4b** illustrate that the difference between the probabilities of failure for different values of ρ for the same value of F_s is greater in **Figure 4b** ($COV_{su} = 0.2$). This result is clearer in **Figures 5a** and **5b** where the ratio of probability of failure for $-0.7 < \rho < 0.7$ to the probability of failure corresponding to $\rho = 0$ is plotted for $COV_{su} = 0.5$ and $COV_{su} = 0.2$, respectively. The probability of failure corresponding to $\rho = 0$ is taken from **Figure 2** with $COV_\gamma = 0.1$. It can be seen that the difference between normalized probabilities of failure for the same value of F_s and for different values of ρ in **Figure 5a** is lower than the same case in **Figure 5b**. For example, in **Figure 5a** for $F_s = 2$, the highest value of P_f/P_f ($\rho = 0$) is 1.28 and the lowest is 0.66, while in **Figure 5b** for the same value of F_s, the highest value of P_f/P_f ($\rho = 0$) is 6.7 and the lowest is about zero.

The shaded region in **Figure 2** corresponds to the practical range of COV_{su} and COV_γ as mentioned in the previous section. For cases where there is a correlation between undrained cohesive soil strength (s_u) and soil unit weight, it is expected that this correlation is positive (i.e. $\rho > 0$) (**Chowdhury and Xu 1992; Sivakumar Babu and Srivastava 2007**). **Figure 6a** shows two sets of curves. The curves with symbols correspond to probability of failure versus factor of safety for lognormal distributed uncorrelated random values of cohesion and unit weight (**Figure 2** with $COV_\gamma = 0.1$). The nearest lower dashed curve corresponds to the same distribution of random lognormal cohesion and unit weight values but with cross-correlation coefficient $\rho = 0.7$. As before, probability of failure decreases for increasing positive cross-correlation coefficients and $F_s > 1$, and the influence of positive cross-correlation on probability of failure is greater for lower values of COV_{su}. The results of the same analyses are presented in **Figure 6b** using reliability index (β).

Numerical solution of c-ϕ soil slopes

Figure 7 shows the model used to investigate the influence of cross-correlation between soil parameters on probability of failure for simple soil slopes with c-ϕ soil strength properties. Mean values of soil properties shown in **Figure 7** were kept the same in numerical calculations. The only deterministic parameter that was changed was the slope angle (α). Probability of failure was calculated for four different values of (mean) factor of safety and for different combinations of

cross-correlation coefficient for pairs of soil parameters. Factor of safety (F_s) and probability of failure (P_f) were calculated using the coupled Simplified Bishop's analysis method and Monte Carlo simulation described earlier.

In these examples, the input parameters (c, ϕ and γ) were assigned values of coefficient of variation which are estimated upper limits, i.e. $COV_c = 0.5$, $COV_\phi = 0.2$ and $COV_\gamma = 0.1$ (**Phoon and Kulhawy 1999**).

Figure 8 shows the influence of cross-correlation between cohesion and friction angle. The values of probability of failure for the same mean values of factor of safety and values of $\rho_1 = -0.5, 0, 0.5$ are presented in this figure. The choice of -0.5 and 0.5 was made because these values fall in the middle of the range of values reported by **Sivakumar Babu and Srivastava (2007)**. For $F_s > 1$, the curve with a negative cross-correlation coefficient value has the lowest probability of failure and the curve with positive cross-correlation has the highest probability of failure. For example, for $F_s = 1.21$ the curve with positive cross-correlation between c and ϕ gives $P_f = 30\%$ and the case with negative cross-correlation corresponds to $P_f = 14.5\%$. However, for $F_s < 1$, the trend is reversed. This is due to changes in the area under the distribution curve of the mean factor of safety when the mean value of the factor of safety is located on the right- or left-hand side of $F_s = 1$. **Griffiths et al. (2009)** also noted that increasing the correlation between c and ϕ will always increase P_f if $P_f < 0.5$ and increasing the correlation between c and ϕ will always decrease P_f if $P_f > 0.5$. A detailed explanation can also be found in the paper by **Javankhoshdel and Bathurst (2014)**. **Allahverdizadeh et al. (2015)** showed the same effect for $P_f < 0.5$ and a range of spatial correlation length using the random finite element method (RFEM).

For the case of a negative cross-correlation between c and ϕ (which is most likely based on the literature), the probability of failure is lower. These results are qualitatively the same as those presented by **Javankhoshdel and Bathurst (2014)** who used the commercially available program SVSlope (**Fredlund and Thode 2011**) to investigate the effect of negative cross-correlation between soil strength parameters on probability of failure (see dashed curve in **Figure 8**). The results of positive cross-correlation between c and ϕ, presented in **Figure 8** are

consistent with **Le (2014)** who noted that if c and ϕ are perfectly positive cross-correlated, the probability of failure increases compared to the case where there is no cross-correlation; this was attributed to dominant occurrences of local failure mechanisms over global failure mechanisms. However, at the time of this study program SVSlope is restricted to cases with cross-correlation between soil cohesion and friction angle only. To investigate the influence of cross-correlation between c and γ and ϕ and γ, the numerical code developed by the writers was used.

Figure 9 presents the effect of different combinations of the values of ρ_1, ρ_2 and ρ_3 on probability of failure for the same mean values of the factor of safety for the c-ϕ slope in **Figure 7**. The dashed line corresponds to cases with uncorrelated input parameters. For simplicity, $\rho_2 = \rho_3$ (cross-correlation between c and γ, and ϕ and γ are the same). Positive cross-correlations between c and γ and between ϕ and γ have been reported in the literature as mentioned in the introduction. However, negative values of $\rho_2 = \rho_3$ and positive values of ρ_1 were also investigated in this study to identify trends. It can be seen in this figure that values of $\rho_1 = -0.5$ and $\rho_2 = \rho_3 = 0.5$ gave the lowest probability of failure, while cases with other values of cross-correlation (e.g. $\rho_1 = 0.5$ and $\rho_2 = \rho_3 = -0.5$) resulted in higher probability of failure. For example, for the value of $F_s = 1.21$, the case with $\rho_1 = -0.5$ and $\rho_2 = \rho_3 = 0.5$ corresponds to $P_f = 9\%$, while the case with $\rho_1 = 0.5$ and $\rho_2 = \rho_3 = -0.5$ gives $P_f = 31\%$. Therefore, for the more reasonable case of negative cross-correlation between c and ϕ and positive cross-correlation between the other pairs of soil parameters, the lowest probability of failure was computed for all $F_s > 1$.

In **Figure 9**, excluding the curves with the highest and lowest probability of failure, the curve with $\rho_1 = \rho_2 = \rho_3 = -0.5$ has the lowest probability of failure (e.g. for $F_s = 1.21$, $P_f = 19\ \%$) compared to the case with no correlation (e.g. for $F_s = 1.21$, $P_f = 25\%$) and the case with $\rho_1 = \rho_2 = \rho_3 = +0.5$ (e.g. for $F_s = 1.21$, $P_f = 29\%$). This implies that the cross-correlation between c and ϕ controls the value of the probability of failure provided that COV_c and COV_ϕ are higher than COV_γ. For this case, ρ_1 has greater influence on the probability of failure.

Figure 9 considers only the example slope case in **Figure 7** and therefore is not general. Furthermore, $\rho_1 = -0.5$, $\rho_2 = \rho_3 = 0.5$ are not the highest absolute values reported in literature. **Figures 10** through **15** are simplified probabilistic stability design charts for the general case of cohesive-frictional (c-ϕ) soils with μ_ϕ = 20, 25, 30, 35, 40 and 45 degrees and values of the cross-correlation coefficient equal to $\rho_1 = -0.7$, $\rho_2 = \rho_3 = 0.7$. These cross-correlation values are the maximum values reported in the literature and thus give the lowest value of the probability of failure. They are very close to the values used by **Sivakumar Babu and Srivastava (2007).** They are used in these new charts to show the maximum difference between probabilities of failure with and without cross-correlation between input parameters.

Figures 10 through **15** are similar to probabilistic slope stability design charts for c-ϕ soil slopes published by **Javnkhoshdel and Bathurst (2014**) which assumed no cross-correlation between soil parameters. These new charts complement the series of previous charts by the writers by including the influence of maximum cross-correlation between parameters. The calculation of F_s remains unchanged from the previous charts by the writers.

The solid contour lines in **Figures 10** through **15** correspond to probability of failure for upper-bound values of spread in soil input values assumed as $COV_c = 0.5$, $COV_\phi = 0.2$ and $COV_\gamma = 0.1$ and uncorrelated soil property values. These curves are very similar to the previous charts by the writers with the exception that in the earlier charts $COV_\gamma = 0$. The difference in numerical outcomes is negligible for the uncorrelated parameter cases. Superimposed on these plots are the red dashed contour lines that correspond to the probability of failure for upper-bound values of COV_c and COV_ϕ and COV_γ with negative cross-correlation between c and ϕ, and a positive cross-correlation between c and γ, and ϕ and γ ($\rho_1 = -0.7$, $\rho_2 = \rho_3 = 0.7$).

The advantage of **Figures 10** through **15** over the earlier charts by the writers is that the influence of uncorrelated and highly correlated soil strength parameters on the probability of failure for simple slopes with the same mean value of the factor of safety is easily detectable. Probability of failure for other combinations of cross-correlation coefficients will fall between the two limiting (upper-bound and lower-bound) cases in these charts.

CONCLUSIONS

The influence of the magnitude of cross-correlation between lognormal distributed random values of undrained shear strength (s_u) and bulk unit weight (γ) on probability of failure was investigated in this paper for the case of simple unreinforced slopes. The closed-form solution reported by **Javankhoshdel and Bathurst (2014)** and **Griffiths and Fenton (2004)** was extended to include the cross-correlation coefficient (ρ) between undrained cohesive strength and unit weight. A numerical code for the solution of the coupled Simplified Bishop's circular slip method and Monte Carlo simulation was used to examine the influence of cross-correlation between lognormal distributed random values of c, ϕ and γ. The same code was used to verify the accuracy of the closed-form solution for the case of cohesive soil slopes.

The main conclusions and contribution of this paper to probabilistic analysis of simple slopes are summarized below:

1. The magnitude of probability of failure is of most interest for cases when the traditional factor of safety is positive but close to one. For these cases the assumption of uncorrelated random variables of undrained cohesive strength (s_u) and (γ) for cohesive slopes leads to higher probability of failure than may be intuitively expected based on magnitude of factor of safety. For example, for the case of uncorrelated values with $COV_\gamma = COV_{su} = 0.1$ and $F_s = 1.3$, the probability of failure is $P_f = 3.5\%$ (**Figure 2**) which is counter intuitive (i.e. too high). However, for the same conditions and cross-correlated random values giving $\rho = +0.7$, the result is $P_f = 0.04\%$ (1/2500) which is judged to be more reasonable. Hence, an important conclusion from this work is that positive correlation between s_u and γ is a possible explanation for the apparent discrepancy in expected margins of safety using conventional deterministic slope stability methods with low but safe values of F_s, and margins of safety expressed probabilistically.

2. **Javankhoshdel and Bathurst (2014)** created a series of probabilistic design charts for simple slopes with uncorrelated random values of c, ϕ and γ. Cross-correlation between random variables can be quantified by the cross-correlation coefficient ρ and this coefficient

introduced into numerical codes. An important contribution of this paper is the formulations that are necessary to compute cross-correlated random values of c, ϕ and γ that have lognormal distributions. These equations are expressed with conventional statistical quantities of mean and coefficient of variation (COV) and can be used directly in coupled slope stability analysis and Monte Carlo simulations. Using the methodology presented in the paper, six different probabilistic slope stability design charts for six different values of friction angle similar to the charts published by **Javankhoshdel and Bathurst (2014)** are presented. However, these new charts complement the earlier series of charts by considering the influence of upper-bound values of COV_c, COV_ϕ and COV_γ representing the spread in random variability of soil input parameters plus the influence of maximum likely cross-correlation between soil parameters.

3. The paper demonstrates that for cases where large probabilities of failure are computed using uncorrelated random input values, the decrease or increase in probability of failure is not of practical concern (i.e. P_f values are very high). However, the paper demonstrates scenarios where P_f using uncorrelated random values gives an unsatisfactory (high) probability of failure but introduction of practical values of cross-correlation between input values leads to a lower P_f value which is safer (i.e. for $P_f < 0.5$ and negative cross-correlation between c and ϕ, and a positive cross-correlation between c and γ, and ϕ and γ).

4. A practical outcome from this study is that the original simplified probabilistic slope stability charts by the writers for cohesive and cohesive-frictional cases based on uncorrelated soil properties (**Javankhoshdel and Bathurst 2014**) are conservative (safe) for design.

There are important limitations to the results presented in this paper. As noted in the introduction, spatial variability of soil properties is not considered. A preliminary quantitative appreciation of the influence of spatial variability on computed probability of failure for simple slopes with uncorrelated soil parameters has been explored in the companion paper by the writers (**Javankhoshdel and Bathurst 2014**). Finally, it should be noted that the range in magnitude of cross-correlation parameters used in analyses has been based on maximum values reported in the literature. However, there is a lack of physical data to justify the range. Nevertheless, using a

wide range of cross-correlation coefficients proved useful to identify trends in analysis outcomes.

ACKNOWLEDGMENTS

Financial support for this research was provided by the Natural Sciences and Engineering Research Council of Canada (NSERC).

REFERENCES

Allahverdizadeh, P., Griffiths, D. and Fenton, G. 2015. The Random Finite Element Method (RFEM) in probabilistic slope stability analysis with consideration of spatial variability of soil properties. In the proceedings of the International Foundations Congress and Equipment Expo 2015 (IFCEE 2015), San Antonio, Texas. American Society of Civil Engineers, pp. 1946-1955.

Ang, A.H. and Tang, W.H. 1984. Probability concepts in engineering planning and design. Vol. 2. Wiley, New York.

Baker, R. 2003. A second look at Taylor's stability chart. ASCE Journal of Geotechnical Geoenvironmental Engineering 129(12): 1102-1108.

Cherubini, C. 1997. Data and considerations on the variability of geotechnical properties of soils. In proceedings of the International Conference on Safety and Reliability (ESREL97), Lisbon, 2: 1583-1591.

Cherubini, C. 2000. Reliability evaluation of shallow foundation bearing capacity on c, ϕ soils. Canadian Geotechnical Journal 37: 264-269.

Ching, J. and Phoon, K.K. 2012. Modeling parameters of structured clays as a multivariate normal distribution. Canadian Geotechnical Journal 49(5), 522-545

Chowdhury, R.N. and Xu, D.W. 1992. Reliability index for slope stability assessment - two methods compared. Reliability Engineering and Systems Safety, 37: 99-108.

Chowdhury, R.N. and Xu, D.W. 1993. Rational polynomial technique in slope reliability analysis. ASCE Journal of Geotechnical Geoenvironmental Engineering 119(12): 1910-1928.

Forrest, W.S. and Orr, T.L. 2010. Reliability of shallow foundations designed to Eurocode 7. Georisk 4(4): 186-207.

Fredlund, M.D. and Thode, R. 2011. SVSlope Theory Manual, SoilVision Systems Inc., Saskatoon, Saskatchewan, Canada.

Griffiths, D.V. and Fenton, G.A. 2004. Probabilistic slope stability analysis by finite elements. ASCE Journal of Geotechnical Geoenvironmental Engineering 130(5): 507-518.

Griffiths, D.V., Huang, J.S. and Fenton, G.A. 2009. Influence of spatial variability on slope reliability using 2-D random fields. ASCE Journal of Geotechnical and Geoenvironmental Engineering 135 (10): 1367–1378.

Hata, Y., Ichii, K. and Tokida, K. 2012. A probabilistic evaluation of the size of earthquake induced slope failure for an embankment. Georisk 6(2): 73-88.

Javankhoshdel, S. and Bathurst, R.J. 2014. Simplified probabilistic slope stability design charts for cohesive and c-ø soils. Canadian Geotechnical Journal 51(9): 1033-1045.

Le, T.M.H. 2014. Reliability of heterogeneous slopes with cross-correlated shear strength parameters. Georisk 8(4): 250-257.

Low, B.K. and Tang, W.H. 1997. Probabilistic slope analysis using Janbu's generalized procedure of slices. Computers and Geotechnics 21(2): 121-142.

Lumb, P. 1970. Safety factors and the probability distribution of soil strength. Canadian Geotechnical Journal 7: 225-242.

Matsuo, M. and Kuroda, K. 1974. Probabilistic approach to design of embankments. Soils and Foundations 14: 1-17.

Michalowski, R.L. 2002. Stability charts for uniform slopes. ASCE Journal of Geotechnical Geoenvironmental Engineering 128(4): 351-355.

Nguyen, V.U. and Chowdhury, R.N., 1985. Simulation for risk analysis with correlated variables. Geotechnique 35(1): 47-58.

Parker, C., Simon, A. and Thorne, C.R. 2008. The effects of variability in bank material properties on riverbank stability: Goodwin Creek, Mississippi. Geomorphology 101: 533-543.

Phoon, K.K. and Kulhawy, F.H. 1999. Characterization of geotechnical variability. Canadian Geotechnical Journal 36(4): 612-624.

Sivakumar Babu, G.L. and Srivastava, A. 2007. Reliability analysis of allowable pressure on shallow foundation using response surface method. Computers and Geotechnics 34(3): 187-194.

Steward, T., Sivakugan, N., Shukla, S.K. and Das, B.M. 2011. Taylor's slope stability charts revisited. ASCE Journal of Geotechnical Geoenvironmental Engineering 11(4): 348-352.

Taylor, D.W. 1937. Stability of earth slopes. J. Boston Soc. Civ. Eng. 24(3): 197-246.

Wu, X.Z. 2013. Trivariate analysis of soil ranking-correlated characteristics and its application to probabilistic stability assessments in geotechnical engineering problems. Soils and Foundations 53(4): 540-556.

Yuceman, M.S., Tang, W.H. and Ang, A.H.S. 1973. A probabilistic study of safety and design of earth slopes. Civil Engineering Studies, Structural Research Series 402, University of Illinois, Urbana, Ill.

LIST OF FIGURES

Figure 1. Taylor's slope stability chart for cohesive soils (**Taylor 1937**).

Figure 2. Probability of failure (P_f) versus (deterministic) mean factor of safety ($\bar{F}_s$) for cohesive soil slopes with lognormal distribution of uncorrelated undrained shear strength (s_u) and unit weight (γ). Note: Shaded region is the practical range. Dashed lines are for cases with $COV_\gamma = 0$ (from **Javankhoshdel and Bathurst 2014**).

Figure 3. a) probability of failure (P_f) and b) reliability index (β) versus (deterministic) mean factor of safety ($\bar{F}_s$) for cohesive soil slopes with lognormal distribution of correlated undrained shear strength (s_u) and unit weight (γ), a range of cross-correlation coefficient (ρ), $COV_{su} = 0.1$, 0.5 and 4, and $COV_\gamma = 0.1$.

Figure 4. Effect of cross-correlation coefficient (ρ) on probability of failure for different mean values of factor of safety and a) $COV_{su} = 0.5$ and b) $COV_{su} = 0.2$ using closed-form solution (solid lines) and numerical results using Monte Carlo simulation (dashed lines). Note: $COV_\gamma = 0.1$.

Figure 5. Effect of cross-correlation coefficient (ρ) on normalized probability of failure for different mean values of factor of safety with $COV_\gamma = 0.1$ and a) $COV_{su} = 0.5$ and b) $COV_{su} = 0.2$.

Figure 6. a) Probability of failure (P_f) and b) reliability index (β) versus (deterministic) mean factor of safety ($\bar{F}_s$) for cohesive soil slopes with lognormal distribution of undrained shear strength (s_u) and unit weight (γ) and a range of COV_{su}. Note: Lines with symbols correspond to $\rho = 0$. Each nearest dashed line is the matching curve with $\rho = 0.7$.

Figure 7. Example slope model geometry and mean soil property values for c-ϕ soil slope example.

Figure 8. Influence of cross-correlation between c and ϕ on probability of failure of the slope in Figure 7 with mean values of c, ϕ and γ shown in the figure.

Figure 9. Effect of different combinations of ρ_1, ρ_2 and ρ_3 on the probability of failure in c-ϕ slopes. Parameter ρ_1 is the cross-correlation coefficient between c and ϕ, ρ_2 is the cross-correlation coefficient between c and γ and ρ_3 is the cross-correlation coefficient between ϕ and γ.

Figure 10. Probabilistic slope stability design chart for μ_ϕ = 20 degrees and COV_c = 0.5, COV_ϕ = 0.2 and COV_γ = 0.1 with $\rho_1 = \rho_2 = \rho_3 = 0$ and ρ_1 = -0.7, $\rho_2 = \rho_3$ = 0.7.

Figure 11. Probabilistic slope stability design chart for μ_ϕ = 25 degrees and COV_c = 0.5, COV_ϕ = 0.2 and COV_γ = 0.1 with $\rho_1 = \rho_2 = \rho_3 = 0$ and ρ_1 = -0.7, $\rho_2 = \rho_3$ = 0.7.

Figure 12. Probabilistic slope stability design chart for μ_ϕ = 30 degrees and COV_c = 0.5, COV_ϕ = 0.2 and COV_γ = 0.1 with $\rho_1 = \rho_2 = \rho_3 = 0$ and ρ_1 = -0.7, $\rho_2 = \rho_3$ = 0.7.

Figure 13. Probabilistic slope stability design chart for μ_ϕ = 35 degrees and COV_c = 0.5, COV_ϕ = 0.2 and COV_γ = 0.1 with $\rho_1 = \rho_2 = \rho_3 = 0$ and ρ_1 = -0.7, $\rho_2 = \rho_3$ = 0.7.

Figure 14. Probabilistic slope stability design chart for μ_ϕ = 40 degrees and COV_c = 0.5, COV_ϕ = 0.2 and COV_γ = 0.1 with $\rho_1 = \rho_2 = \rho_3 = 0$ and ρ_1 = -0.7, $\rho_2 = \rho_3$ = 0.7.

Figure 15. Probabilistic slope stability design chart for μ_ϕ = 45 degrees and COV_c = 0.5, COV_ϕ = 0.2 and COV_γ = 0.1 with $\rho_1 = \rho_2 = \rho_3 = 0$ and ρ_1 = -0.7, $\rho_2 = \rho_3$ = 0.7.

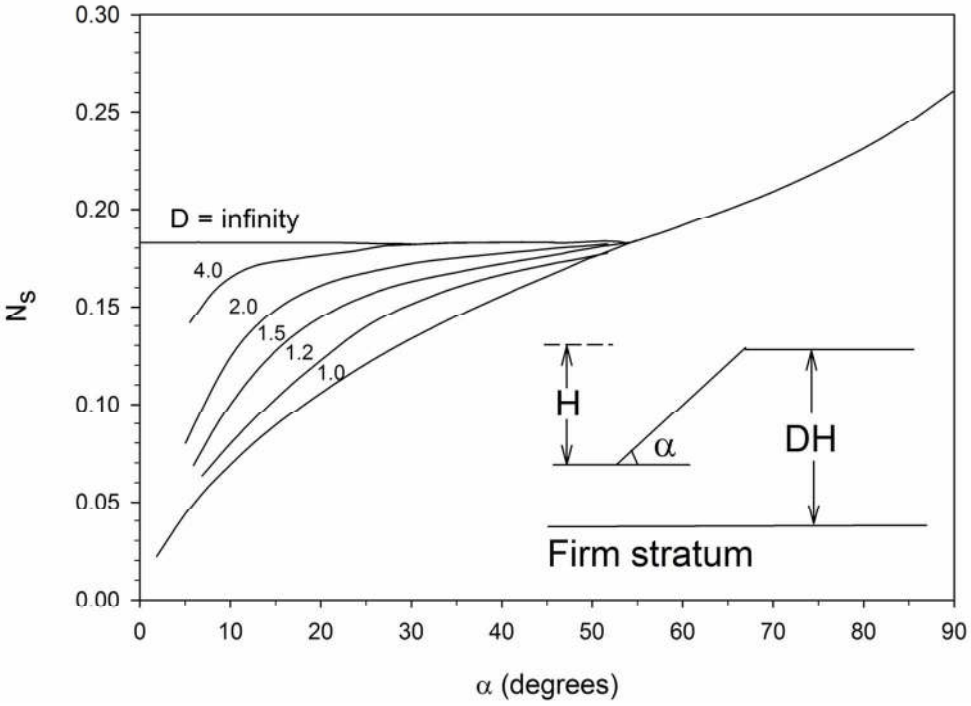

Figure 1. Taylor's slope stability chart for cohesive soils (Taylor 1937).
118x92mm (300 x 300 DPI)

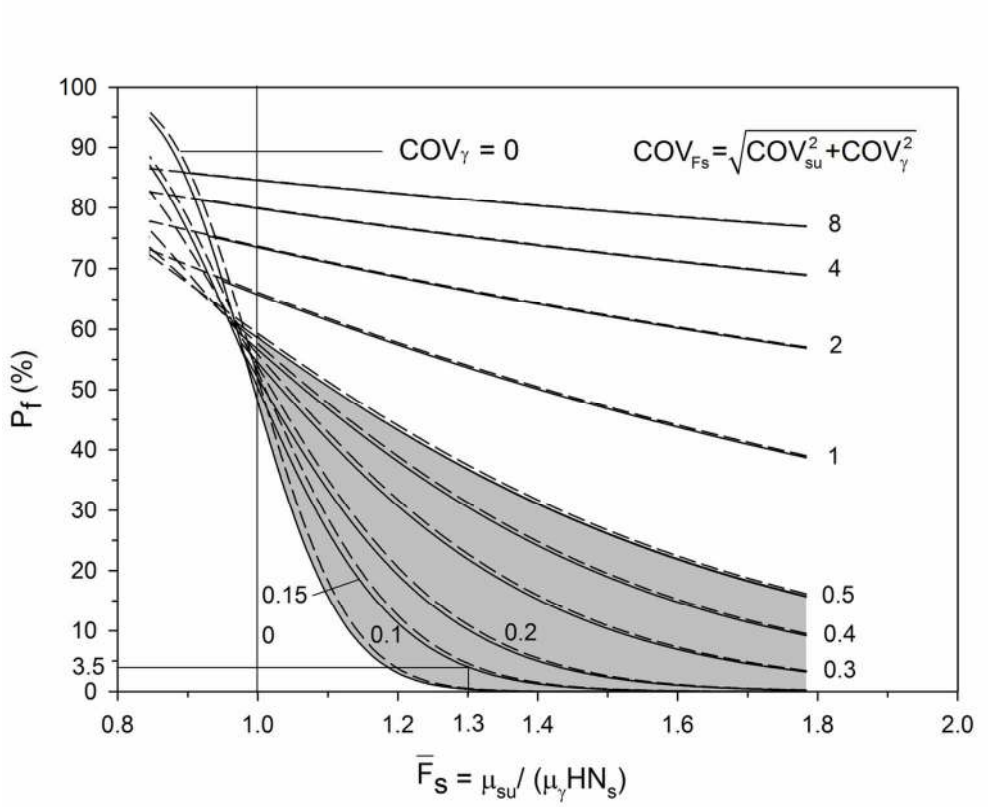

Figure 2. Probability of failure (Pf) versus (deterministic) mean factor of safety ($\overline{F}_s$) for cohesive soil slopes with lognormal distribution of uncorrelated undrained shear strength (su) and unit weight (γ). Note: Shaded region is the practical range. Dashed lines are for cases with $COV_\gamma = 0$ (from Javankhoshdel and Bathurst 2014).
120x97mm (300 x 300 DPI)

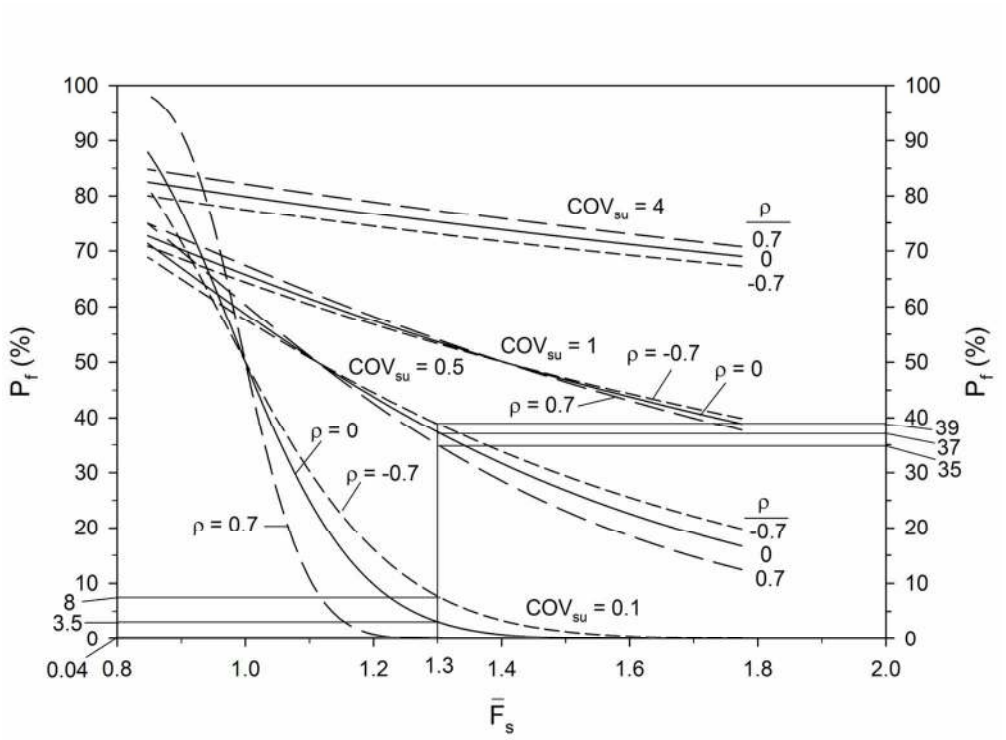

Figure 3. a) probability of failure (Pf)

Figure 3. a) probability of failure (Pf) and b) reliability index (β) versus (deterministic) mean factor of safety ($\bar{F}_s$) for cohesive soil slopes with lognormal distribution of correlated undrained shear strength (su) and unit weight (γ), a range of cross-correlation coefficient (ρ), COVsu = 0.1, 0.5 and 4, and COV_γ = 0.1.
119x88mm (300 x 300 DPI)

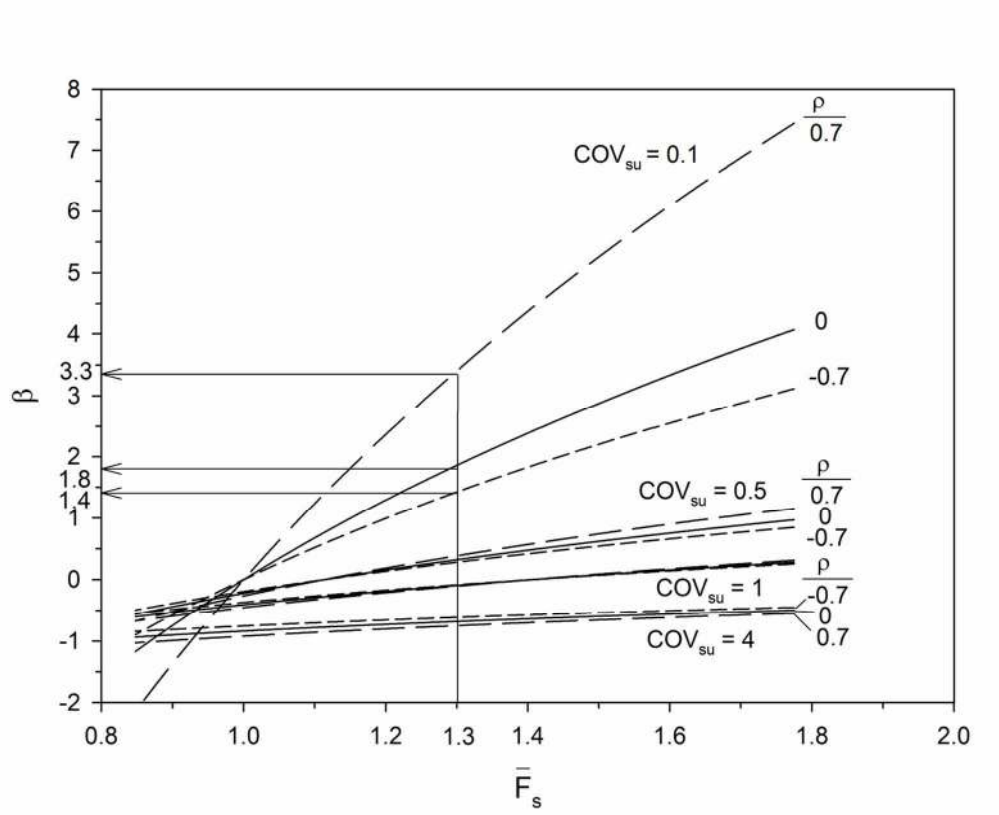

Figure 3. b) reliability index (β)

Figure 3. a) probability of failure (Pf) and b) reliability index (β) versus (deterministic) mean factor of safety ($\bar{F}_s$) for cohesive soil slopes with lognormal distribution of correlated undrained shear strength (su) and unit weight (γ), a range of cross-correlation coefficient (ρ), COVsu = 0.1, 0.5 and 4, and COVγ = 0.1.
119x98mm (300 x 300 DPI)

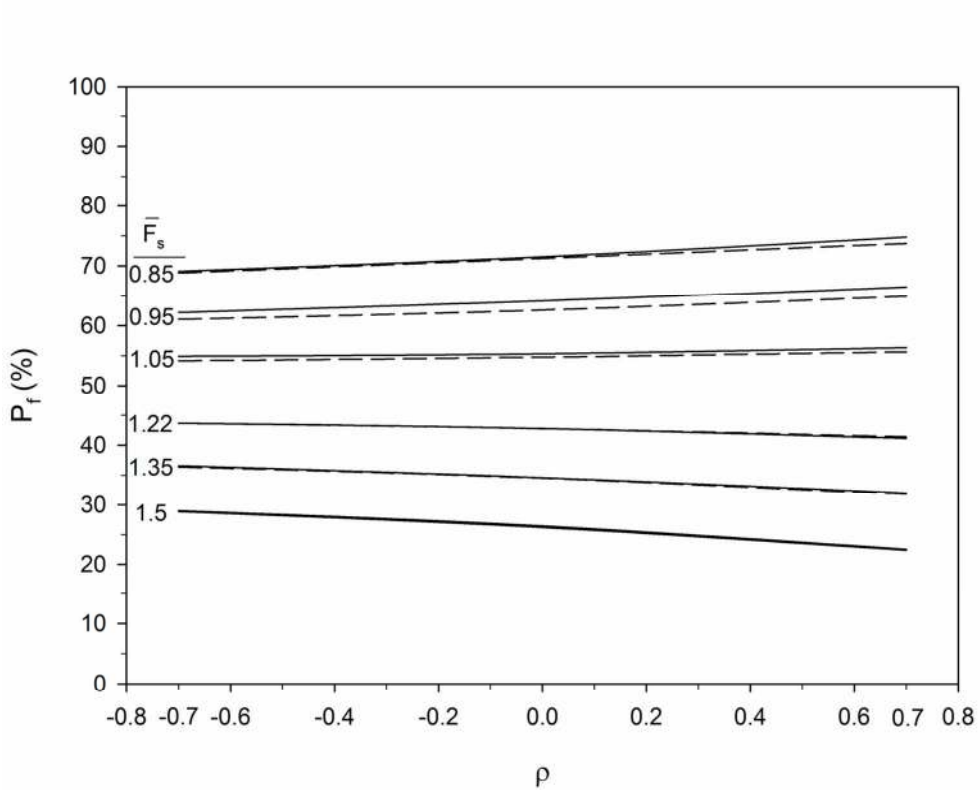

Figure 4.
a) COVsu = 0.5
Effect of cross-correlation coefficient (rho) on probability of failure for different mean values of factor of safety and a) COVsu = 0.5 and b) COVsu = 0.2 using closed-form solution (solid lines) and numerical results using Monte Carlo simulation (dashed lines). Note: COV_Y = 0.1.
118x94mm (300 x 300 DPI)

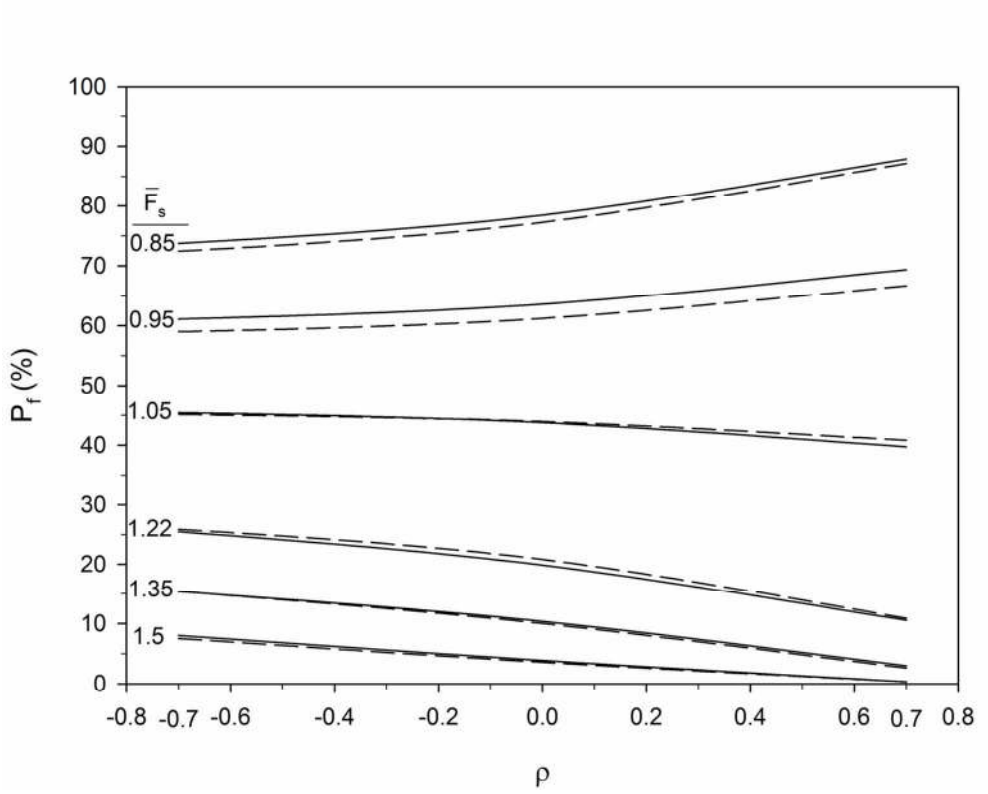

Figure 4.
b) COVsu = 0.2
Effect of cross-correlation coefficient (rho) on probability of failure for different mean values of factor of safety and a) COVsu = 0.5 and b) COVsu = 0.2 using closed-form solution (solid lines) and numerical results using Monte Carlo simulation (dashed lines). Note: COV_Y = 0.1.
118x94mm (300 x 300 DPI)

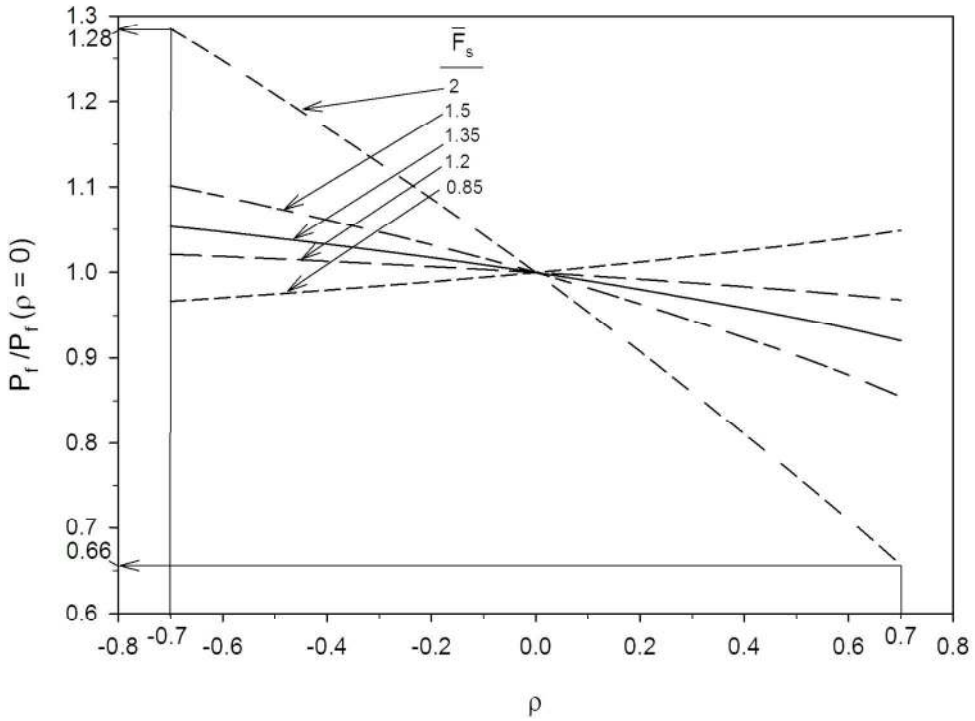

Figure 5.
a) COVsu = 0.5
Effect of cross-correlation coefficient (ρ) on normalized probability of failure for different mean values of factor of safety with COVγ = 0.1 and a) COVsu = 0.5 and b) COVsu = 0.2.
149x118mm (300 x 300 DPI)

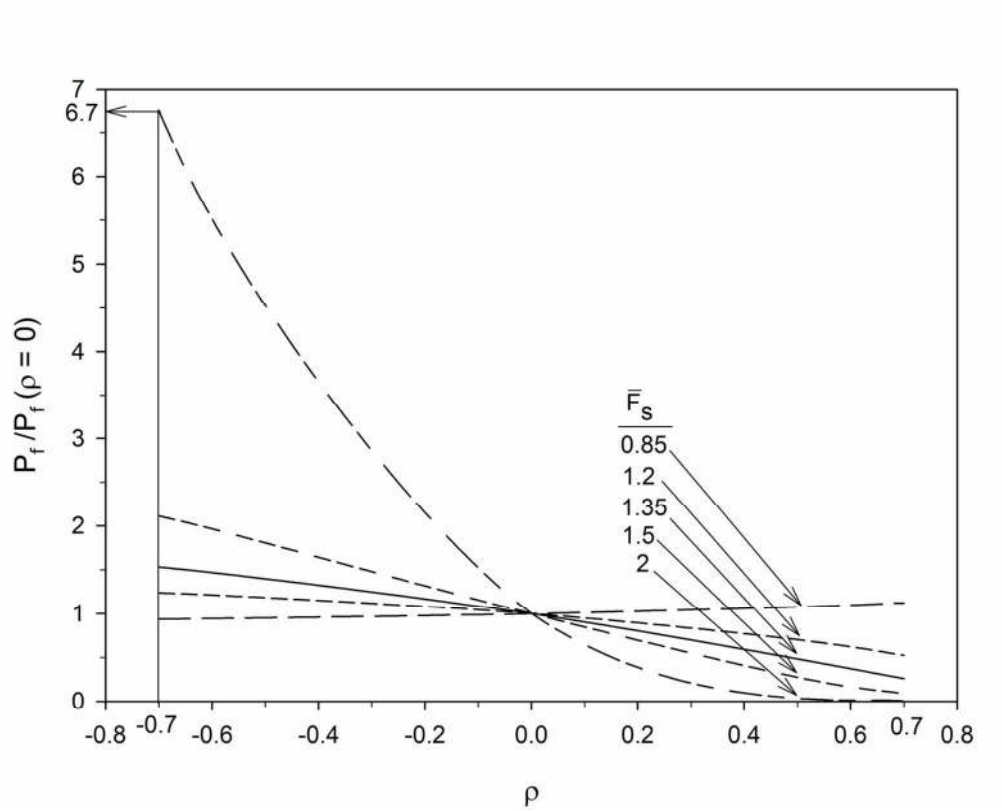

Figure 5.
b) COVsu = 0.2
Effect of cross-correlation coefficient (ρ) on normalized probability of failure for different mean values of factor of safety with COVγ = 0.1 and a) COVsu = 0.5 and b) COVsu = 0.2.
118x96mm (300 x 300 DPI)

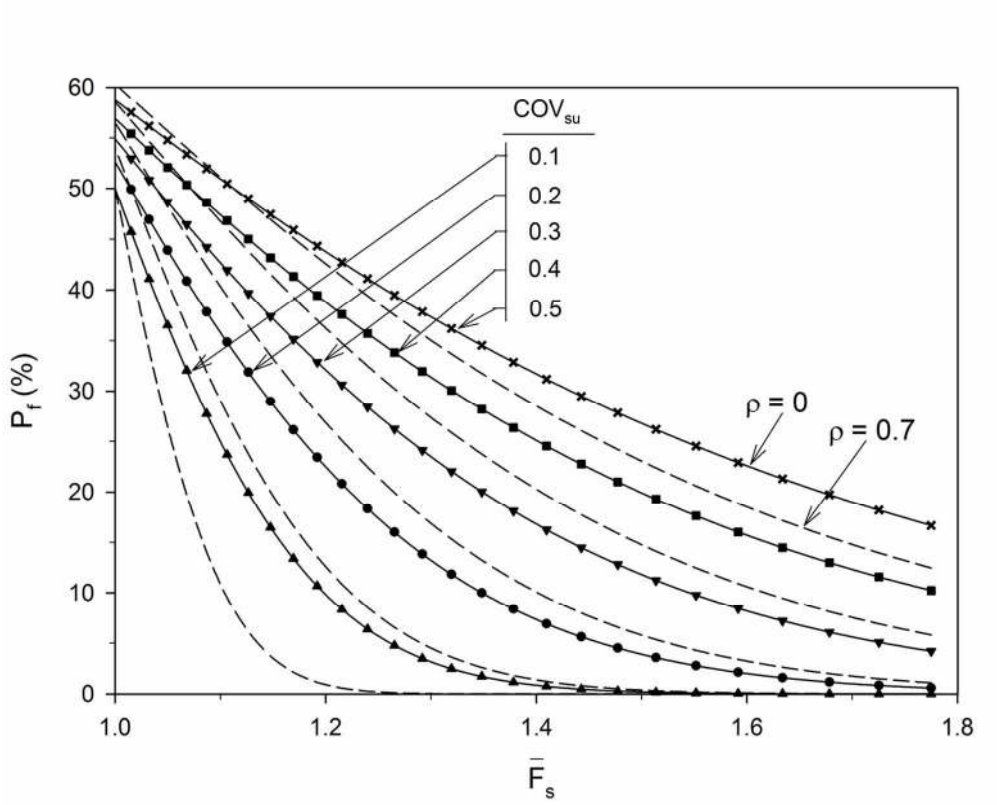

Figure 6.
a) probability of failure (Pf)
a) Probability of failure (Pf) and b) reliability index (β) versus (deterministic) mean factor of safety ($\bar{F}_s$) for cohesive soil slopes with lognormal distribution of undrained shear strength (su) and unit weight (g) and a range of COVsu. Note: Lines with symbols correspond to ρ = 0. Each nearest dashed line is the matching curve with ρ = 0.7.
119x96mm (300 x 300 DPI)

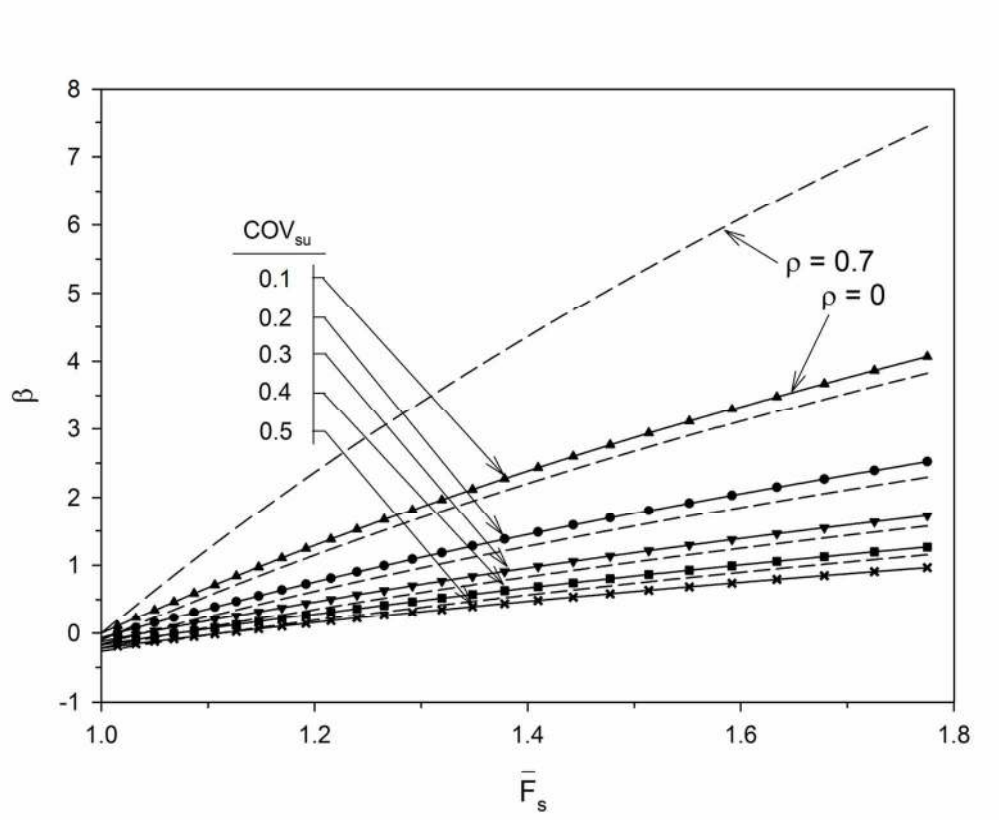

Figure 6.
b) reliability index (β)
a) Probability of failure (Pf) and b) reliability index (β) versus (deterministic) mean factor of safety ($\bar{F}_s$) for cohesive soil slopes with lognormal distribution of undrained shear strength (su) and unit weight (γ) and a range of COVsu. Note: Lines with symbols correspond to ρ = 0. Each nearest dashed line is the matching curve with ρ = 0.7.
120x99mm (300 x 300 DPI)

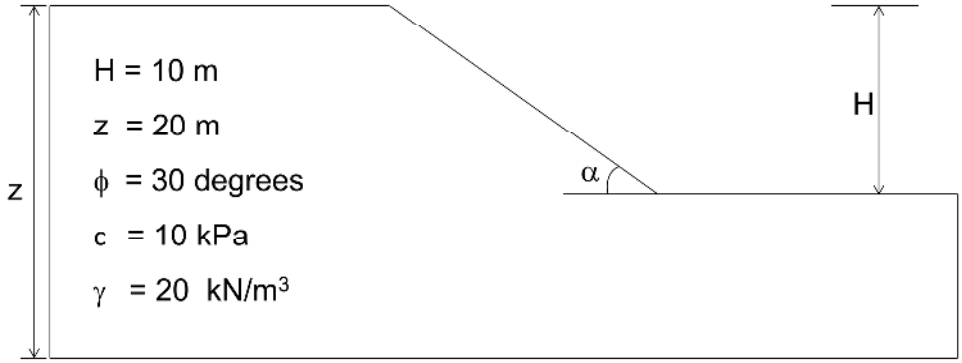

Figure 7. Unreinforced slope model geometry and mean soil property values for c-Φ soil slope example.
190x142mm (300 x 300 DPI)

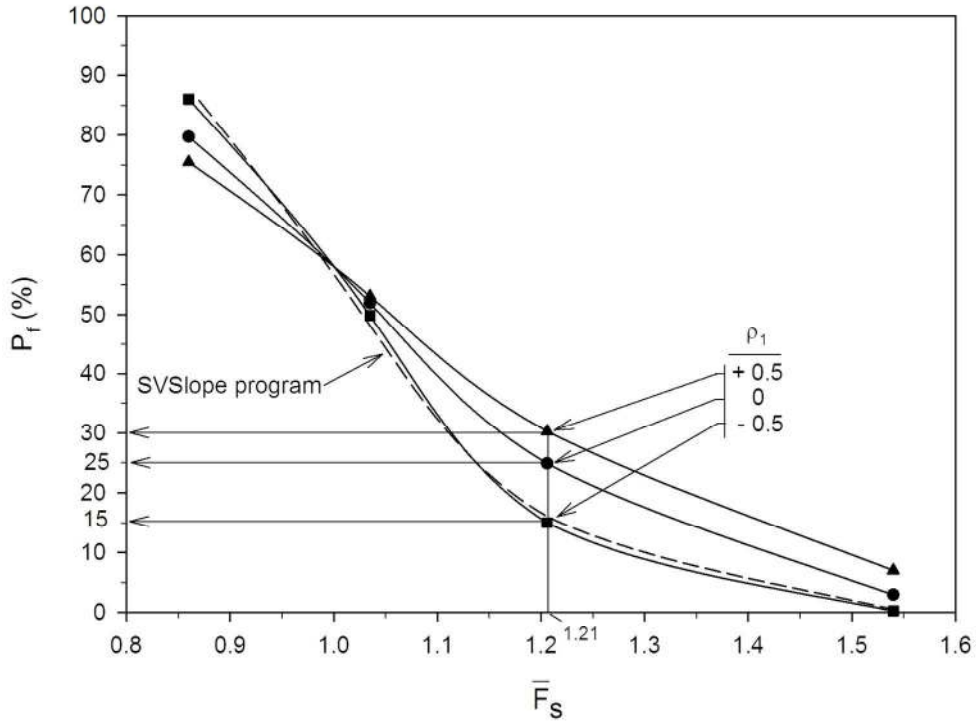

Figure 8. Influence of cross-correlation between c and Φ on probability of failure of the slope in Figure 7 with mean values of c, Φ and γ shown in the figure.
150x120mm (300 x 300 DPI)

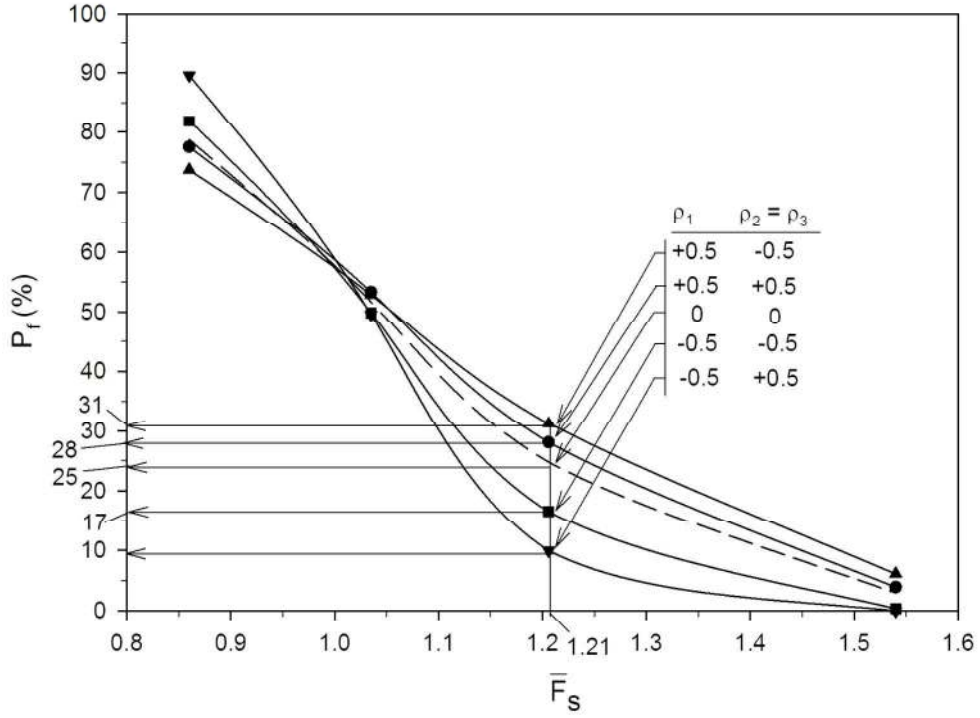

Figure 9. Effect of different combinations of ρ1, ρ2 and ρ3 on the probability of failure in c-Φ slopes. Parameter ρ1 is the cross-correlation coefficient between c and Φ, ρ2 is the cross-correlation coefficient between c and γ and ρ3 is the cross-correlation coefficient between Φ and γ.
150x119mm (300 x 300 DPI)

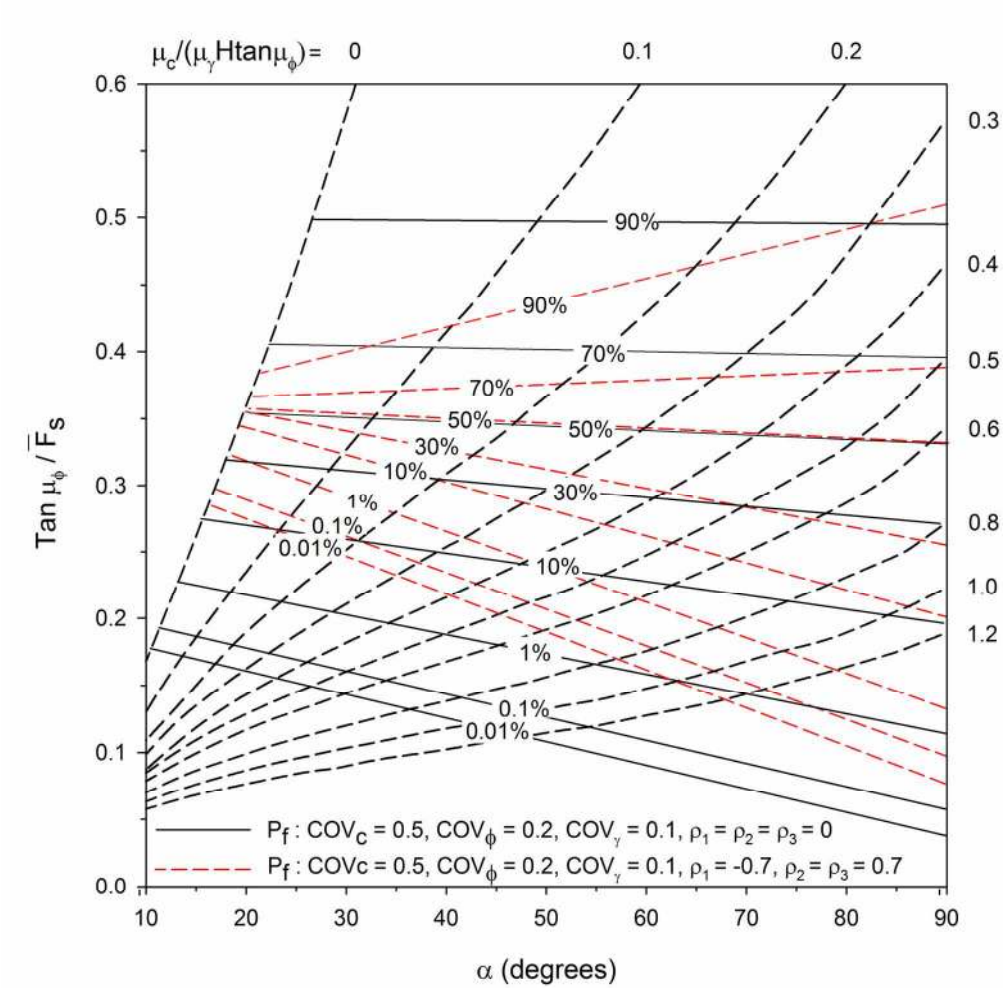

Figure 10. Probabilistic slope stability design chart for μΦ= 20 degrees and COVc = 0.5, COVΦ = 0.2 and COVγ = 0.1 with ρ1 = ρ2 = ρ3 = 0 and ρ1 = -0.7, ρ2 = ρ3 = 0.7.
153x151mm (300 x 300 DPI)

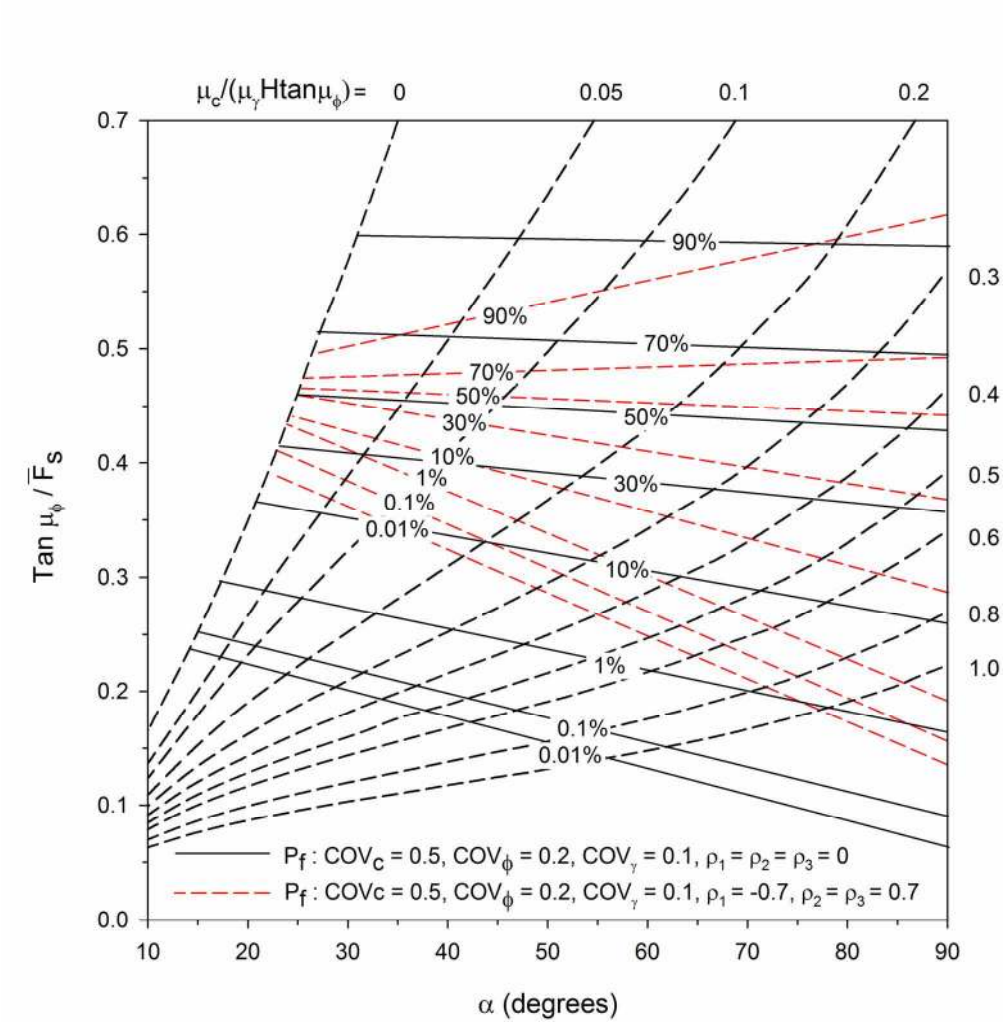

Figure 11. Probabilistic slope stability design chart for μΦ= 25 degrees and COVc = 0.5, COVΦ = 0.2 and COVγ = 0.1 with ρ1 = ρ2 = ρ3 = 0 and ρ1 = -0.7, ρ2 = ρ3 = 0.7.
159x163mm (300 x 300 DPI)

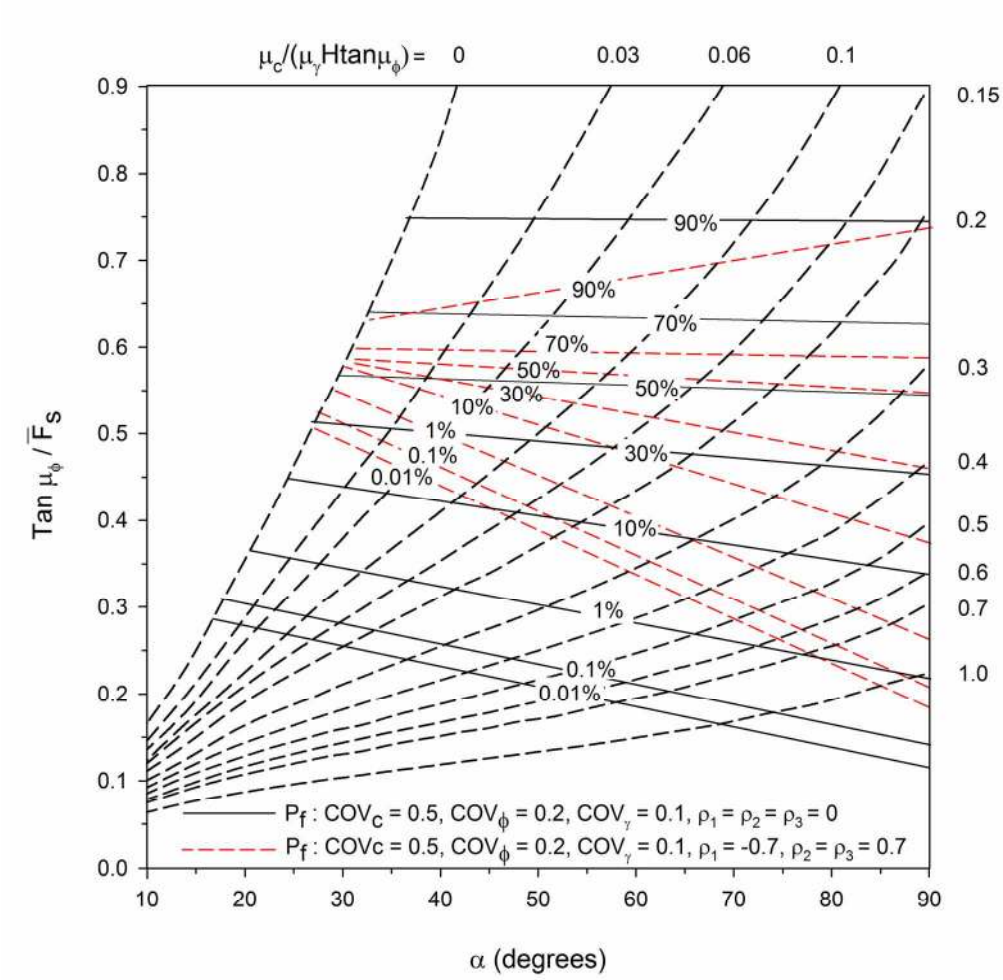

Figure 12. Probabilistic slope stability design chart for μΦ= 30 degrees and COVc = 0.5, COVΦ = 0.2 and COVγ = 0.1 with ρ1 = ρ2 = ρ3 = 0 and ρ1 = -0.7, ρ2 = ρ3 = 0.7.
159x159mm (300 x 300 DPI)

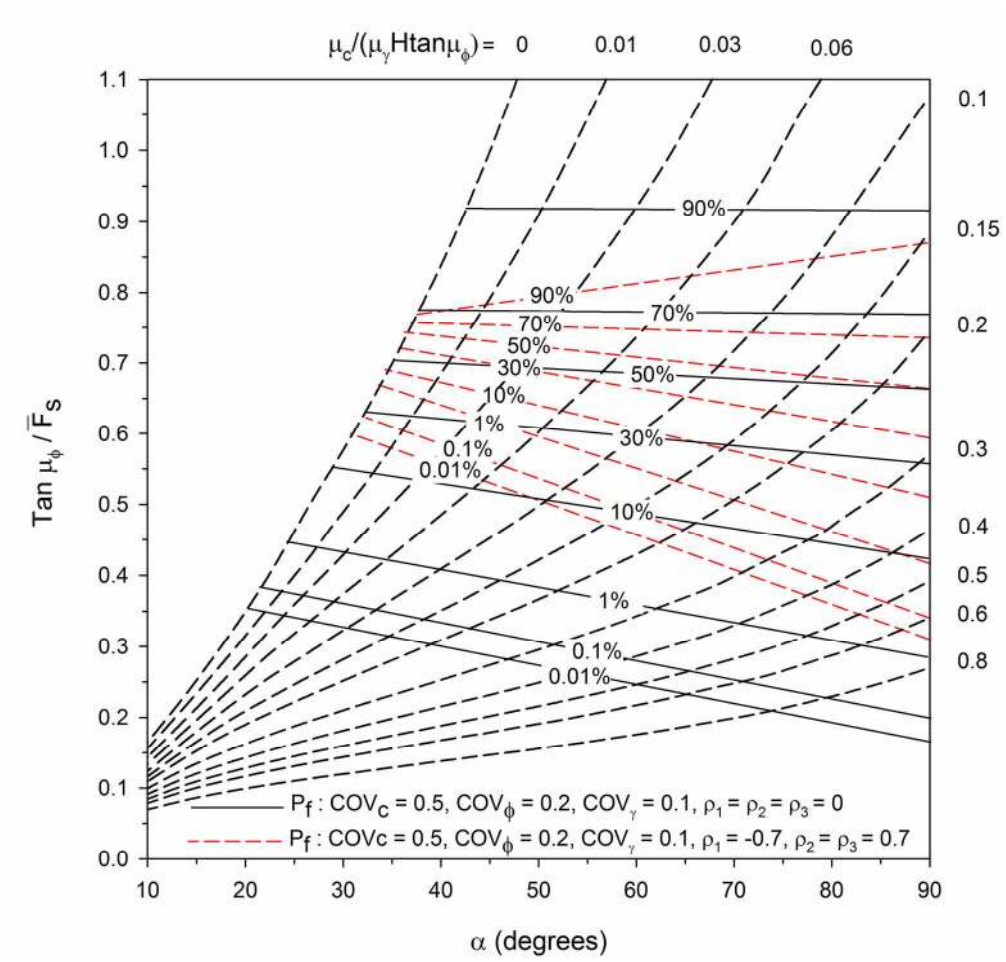

Figure 13. Probabilistic slope stability design chart for μΦ= 35 degrees and COVc = 0.5, COVΦ = 0.2 and COVγ = 0.1 with ρ1 = ρ2 = ρ3 = 0 and ρ1 = -0.7, ρ2 = ρ3 = 0.7.
152x145mm (300 x 300 DPI)

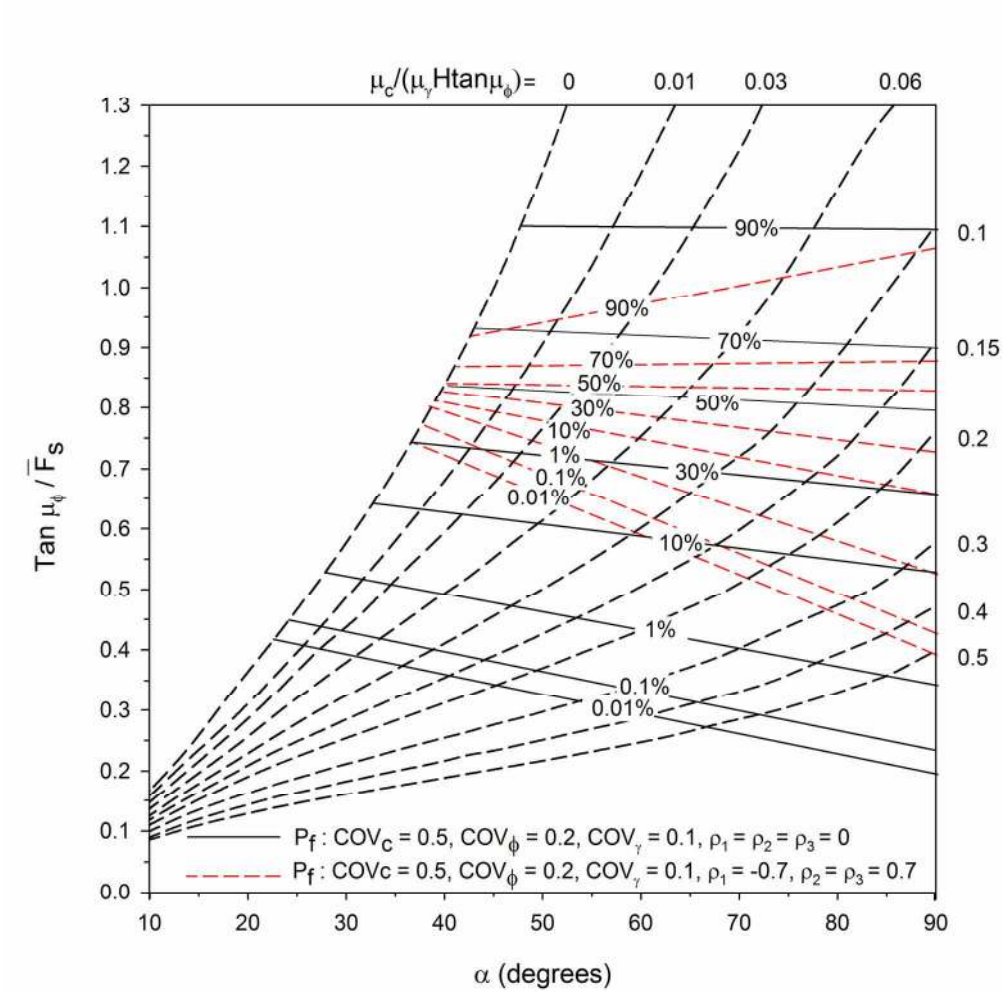

Figure 14. Probabilistic slope stability design chart for μΦ= 40 degrees and COVc = 0.5, COVΦ = 0.2 and COVγ = 0.1 with ρ1 = ρ2 = ρ3 = 0 and ρ1 = -0.7, ρ2 = ρ3 = 0.7.
157x156mm (300 x 300 DPI)

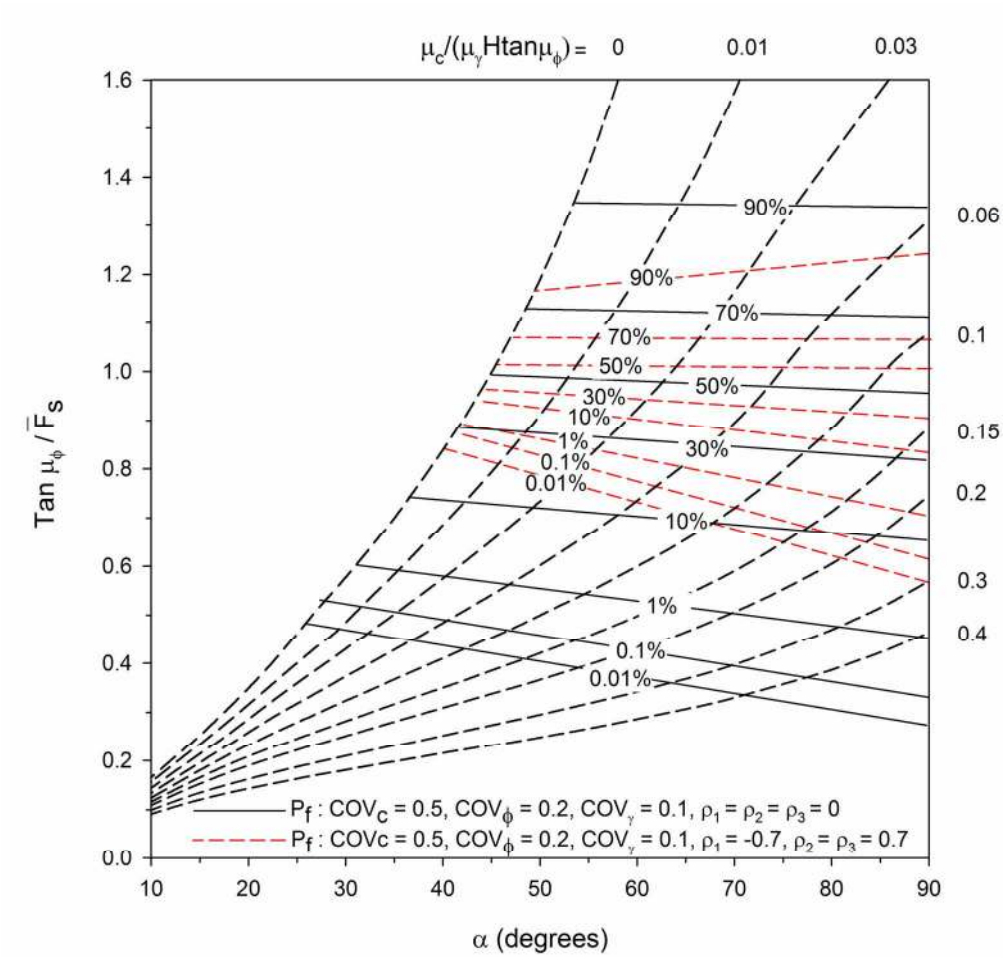

Figure 15. Probabilistic slope stability design chart for μΦ= 45 degrees and COVc = 0.5, COVΦ = 0.2 and COVγ = 0.1 with ρ1 = ρ2 = ρ3 = 0 and ρ1 = -0.7, ρ2 = ρ3 = 0.7.
152x145mm (300 x 300 DPI)